Ocean Sci. Discuss., 9, 2457–2491, 2012
www.ocean-sci-discuss.net/9/2457/2012/
doi:10.5194/osd-9-2457-2012

Ocean Science Discussions

Surface signature of Mediterranean water eddies in the North-East Atlantic: effect of the upper ocean stratification

I. Bashmachnikov[1] **and X. Carton**[2]

[1]Institute of Oceanography of the Faculty of Sciences of the University of Lisbon (OI-FCUL), Campo Grande, 1749-016, Lisbon, Portugal
[2]Laboratoire de Physique des Océans, UMR6523, Université deBretagne Occidentale, 6 avenue Le Gorgeu, 29200 Brest, France

Received: 9 June 2012 – Accepted: 5 July 2012 – Published: 20 July 2012

Correspondence to: I. Bashmachnikov (igorb@fc.ul.pt)

Published by Copernicus Publications on behalf of the European Geosciences Union.

Abstract

Meddies, intra-thermocline eddies of Mediterranean water, are often visible at the sea surface as positive sea-level anomalies. Here we study the surface signature of several meddies tracked with RAFOS floats and AVISO altimetry. Then, theoretical estimates of the surface signature of a meddy are derived, based on geostrophy and potential vorticity balance. The intensity of the surface signature is proportional to the meddy core radius and to the Coriolis parameter, and inversely proportional to the core depth and buoyancy frequency. This indicates that surface signature of a meddy may be strongly reduced by the upper ocean stratification. Estimates suggest that the southernmost limit for detection in altimetry of small meddies (with radii on the order of 15 km) should lie in the northern subtropics, while large meddies (with radii of 25–30 km) could be detected as far south as the northern tropics. During the initial period of meddy acceleration after meddy formation or a stagnation stage, a cyclonic signal also is generated at the sea-surface, but mostly the anticyclonic surface signal follows the meddy.

1 Introduction

Generated by the destabilization of the Mediterranean outflow along the Iberian Peninsula and at surrounding banks, meddies (Mediterranean Water Eddies) drift across the Northeastern Atlantic, sometimes reaching the Mid-Atlantic Ridge without major change of their dynamical properties (Serra and Ambar, 2002; Richardson et al., 2000). Meddies, warm and salty intrathermocline eddies, are isolated from the surrounding waters by strong potential vorticity gradients and show low horizontal and vertical diffusivities (Hebert, 1988; Martin et al., 2001). For meddies, horizontal intrusions are thought to be the most probable mechanism for heat and salt exchange across their lateral boundaries, but they are not an efficient mechanism for vorticity dissipation until the late stages of the eddy disintegration (Hebert, 1988; Hebert et al., 1990). Relative vorticity decay in meddies may be due to their interaction with a background shear

flow, which strips vorticity away (Legras and Dritschel, 1993; Mariotti et al., 1994), or to energy dispersion through radiation of Rossby waves (Flierl, 1984). Core properties of meddies also change when they interact with seamounts. Such interactions can range from "elastic", when the eddy only slightly changes its trajectory, to "drastic", when the eddy is split into several parts or destroyed after interaction with the seamount (Van Geffen and Davies, 2000; Richardson et al., 2000; Bashmachnikov et al., 2009b).

Since the pioneering work by Käse et al. (1989), several in situ surveys of meddies in the Northeastern Atlantic Ocean have shown that these eddies can have a signature at the sea-surface (Pingree and Le Cann, 1993a,b; Pingree, 1995; Tychensky and Carton, 1998; Paillet et al., 2002; etc.) (see Table 1). On average, the azimuthal velocities near the sea-surface are around 70 % of those of the meddy core, varying from 30 to 100 % (Bashmachnikov et al., 2009a). These strong surface signals, and the stability of meddies, allow their possible tracking with altimetry (Armi et al., 1988; Stammer et al., 1991; Pingree and Le Cann, 1993b; Bower et al., 1997; Richardson et al., 2000).

Up to now, no systematic investigation of meddy surface signals, nor of background ocean conditions which can affect their intensity, has been carried out. In this paper we develop criteria to determine where meddies with given characteristics can be observed at the sea-surface.

2 Materials and methods

For the experimental part of this work, we used several available studies which extend from meddy cores to the ocean surface (Table 1). The characteristics of the meddies, their signature at the surface and the background oceanographic conditions form the test bed of the theoretical study to follow. In addition, a joint analysis of RAFOS float trajectories in meddies and of AVISO altimetry data was performed to examine variations of the surface signatures of meddies with time. To study these long-term variations, we retained only the meddies thoroughly surveyed at least once with CTD sections and followed with subsurface drifters for at least several months. Meddies Hyperion, Zoe

(Tychensky and Carton, 1998; Richardson and Tychensky, 1998) and Pinball (Pingree, 1995; Richardson et al., 2000) satisfied those requirements.

For each meddy, the RAFOS floats trajectories were split into rotation cycles; during each cycle, the RAFOS positions were averaged to determine the position of the meddy center. For each cycle, the mean values of the distance between the RAFOS and the meddy centre (called here "the radius"), temperature, azimuthal velocities, and meddy propagation velocities, were estimated. If several RAFOS floats were simultaneously rotating around a meddy centre, the final results represented the average values over all these floats. The results were interpolated and smoothed with piecewise cubic, Hermit interpolation polynomials over 7-day intervals, centred at the same dates as the gridded altimetry data (AVISO).

From the RAFOS float data, the relative vorticity of each meddy was computed, assuming that it had a shielded Gaussian (or Rayleigh) profile (Carton et al., 1989). This hypothesis is reasonable for the radial profile of relative vorticity ω, in view of previous in situ observations (Pingree and Le Cann, 1993a; Paillet et al., 2002), but finer details of real vorticity profiles will be discussed below. The Rayleigh profile is:

$$\omega(r) = \left(2 - \frac{r^2}{R_{\mathrm{vm}}^2}\right) \frac{v_\theta(r)}{r},$$

where R_{vm} is the radius where the azimuthal velocity v_θ reaches its maximum. The values of v_θ and r were derived from float data, averaged over rotation cycles, while R_{vm} was derived from in situ sections across the meddy. The dynamical radii of meddies (R_{m}) were defined as the distance at which the vorticity changed sign. For a Rayleigh profile, the two radii are related by $R_{\mathrm{m}} = \sqrt{2}R_{\mathrm{vm}}$.

Gridded altimetric data with a spatial resolution of about 30 km were used to compute the sea-surface velocity and relative vorticity with the geostrophic approximation. At the surface, meddy signatures were often mixed with other dynamical structures; therefore we identified meddy surface signals from local extrema of the sea-level (Isern-Fontanet et al., 2003). These extrema are given by the Laplacian of sea-level height, proportional

to surface relative vorticity. Note that such extrema can also represent surface eddies. Their correlation with RAFOS float positions was therefore essential.

3 Description of observed meddy surface signals

Table 1 summarizes the simultaneous in situ observations of meddies and of their surface signatures available from literature.

The peak vorticity of the meddies was computed from the Rayleigh model as $\omega_{R_m}(0) = 2\sqrt{e}\frac{V_{\theta\max}}{R_{vm}}$, where R_{vm} and the maximum azimuthal velocity ($v_{\theta\max}$) are derived from observations. In fact, $\omega_m(0)$ directly derived from the experimental distribution of v_θ was 1.2 times smaller than $\omega_{R_m}(0)$. The later correction, further on applied to the results of the Rayleigh model, may be due to the fact that, close to the center, the observed relative vorticity of meddies was most often uniform and thus did not exactly match the Rayleigh profile (see in particular, Richardson et al., 1989; Armi et al., 1989). Observations showed that 3/4 of the presented meddies were coupled to a surface signature with relative vorticity $\omega_0 \sim -0.1f$ (f is the Coriolis parameter); the relative vorticity of the surface signal ranged from 20 to 50 % (on average around 30 %) of that in the meddy core (ω_m). Observations also indicated that the R_{vm} of the surface signature was twice that of the meddy.

For the meddies tracked with RAFOS floats, we fitted the meddy positions with the AVISO altimetry maps. The surface negative vorticity anomalies typically peaked above the centers of the observed meddies (i.e. less than 16 km away), and rarely 16 to 49 km away. The modulus of relative vorticity monotonically decreased to zero over the radial distances of 50 to 100 km (see Figs. 1–3). Nearly all selected meddies were coupled to a noticeable relative vorticity anomaly during 80 to 100 % of the observation time (Table 2). The only exception was meddy Ceres, which did not show a clear surface signature for a significant part of its tracked trajectory. This meddy lost its surface signal while crossing the Azores Current and did not regain it until it got destroyed at the Irving seamount (Richardson et al., 2000).

Meddies Zoe and Hyperion possessed comparable characteristics, were observed at approximately the same latitudes and showed surface signals of similar intensity at the beginning of their registered journey. But their surface signals evolved differently.

Zoe (September 1994–February 1995) drifted westward in a dynamically calm region north of the Azores Current and generated an intense permanent surface signal along its trajectory (Fig. 1a, b). Following an initial decrease, the surface signal remained rather stable up to December–January 1995, when it sharply increased; an increase of the relative vorticity was also registered by the in-core RAFOS float (Fig. 1c). This increase was accompanied by a rapid drift of the RAFOS towards the meddy centre, suggesting strong variations in the shape of its core. The correlation of the mean and minimum relative vorticities of the surface signal with the variations in ω_m of the meddy core (Fig. 1c), as registered by the RAFOS float, reached 0.75–0.77; this suggests a strong influence of the meddy core changes on the surface signal intensity. These strong changes may have been related to an interaction with a bottom rise of Santa Maria island, and/or to an interaction with another meddy. No in situ data are available to identify a meddy north of Zoe, but the meddy may be connected with an anticyclonic surface signal, which was moving southwards along the eastern slope of the San Miguel–Santa Maria plateaux (Fig. 1b). A plausible eddy-eddy interaction might take place in November 1994, when the surface anticyclone was seen in altimetric data north of Zoe at a distance of about 2 meddy diameters. During this period Zoe sharply changed the direction of drift and began a clockwise rotation around the anticyclonic structure to the north. The abovementioned abrupt change in RAFOS characteristics occurred two months later, in January 1995, after Zoe had left the south-eastern tip of the San Miguel-Santa Maria plateaux. Therefore they might rather be a result of merging with another meddy than of topographic origin (Fig. 1a).

Meddy Hyperion (July 1993–December 1994) had a significant southward drift component. In the first year of its registered propagation Hyperion moved from 36 to 27° N (Fig. 2a, b). During this period the meddy interacted with, and crossed the Azores Current. After crossing the Azores Current, it underwent a long-lasting interaction with

a surface cyclone detached from the jet. These two interactions were presumably responsible for the variations of the meddy surface signal during a period shorter than a month (Fig. 2c). During an the initial period, the RAFOS floats in the meddy core showed a fast outward drift, in particular as the meddy interacted with the Plato seamount (Fig. 2a and c, see also Richardson and Tychensky, 1998). Later on (from November 1993 to November 1994), the RAFOS floats rotated at about 30–40 km from the meddy center. During this latter period, the azimuthal velocity and the core temperature showed a slight and gradual decrease with time, suggesting a continuous dissipation of the relative and potential vorticity anomalies of the meddy core (Fig. 2c). At the same time, the variations of the surface signal along the meddy track were more drastic. The mean and maximum surface signal intensity decreased substantially as the meddy rapidly drifted southward: in November 1993, in December–January 1993/1994 and in April–June 1994 (Fig. 2a–c). Approximated with linear trends, the modulus of the mean relative vorticity at the surface, less than 20 km away from the meddy centre, decreased by $3.0 \times 10^{-7}\,s^{-1}$ per month, and of its peak relative vorticity (not shown) – by $3.8 \times 10^{-7}\,s^{-1}$ per month. This is significantly faster than the decrease of the modulus of the peak relative vorticity at the meddy core ($2.3 \times 10^{-7}\,s^{-1}$ per month).

Meddy Pinball (January–September 1994) was first detected shortly after its formation near the Iberian coast (Pingree, 1995). Later on, it propagated westward, merged with another meddy and finally got destroyed at the Josephine seamount (Fig. 3a). At the time of its formation, this meddy was first overlain by a surface cyclone, the formation of which concurred with the formation of the meddy. As the meddy started moving away from the continental slope in January 1994 the cyclonic signal intensified, but did not follow the meddy (Fig. 3b). About a month later, the meddy interacted with the cyclone (Richardson et al., 2000), dived under it and lost its weak anticyclonic surface signal. Finally, in April, the meddy started its travel north and then west, gaining a permanent, though weak, anticyclonic signature at the surface. The signal doubled its mean and peak surface vorticity as Pinball merged with another meddy (Richardson et al., 2000) in May–June 1994 (Fig. 3c).

4 Theoretical estimates of meddy surface signatures

4.1 Homogeneous upper layer

Observations indicate that a drifting meddy, while pushing its way through the water column, raises isopycnals above it (Hebert, 1988; Paillet et al., 2002; Carton et al., 2002). As a consequence of potential vorticity (q) conservation, $q = \frac{f+\omega_0}{\tilde{H}-H_m}$, negative vorticity should be generated in the upper layer, above the front slope of the meddy (Paillet et al., 2002; Bashmachnikov et al., 2009a):

$$\omega_0 = -\frac{\Delta H}{\tilde{H}} f \tag{1}$$

Here $\tilde{H}$ is the mean thickness of the upper layer and H_m is its perturbation by the moving meddy, with maximum value ΔH over the meddy centre (Fig. 4). $\tilde{H}$ is typically 200 m less than H, the depth of the centre of meddy core (Hebert, 1988; Paillet et al., 2002; Carton et al., 2002). Taking characteristic values of $\tilde{H} \sim 700$ m and isopycnal elevations $\Delta H \sim 50$–100 m, the vorticity, generated in the upper layer, will be $\omega \sim -0.07$ to $-0.14f$. This represents 20 to 40 % of a meddy peak vorticity (of about $-0.3f$) and corresponds well to the observations in Table 1. With $f \sim 8 \times 10^{-5}\,s^{-1}$, and a dynamic radius of the surface signature $R \sim 50$ km (Table 2, see also Oliveira et al., 2000; Paillet et al., 2002), the maximum azimuthal velocity at the sea-surface is then $v_\theta \sim \frac{\omega_0 R}{\sqrt{5.5\,e}} \sim 7$–$15\,cm\,s^{-1}$ (compare with Figs. 1–2b).

Dynamically, a moving meddy forces the fluid above its frontal slope to diverge, but the Coriolis acceleration resists the process deflecting the fluid particles from the radial direction. As a result the vertical velocity and the sea-surface doming are induced to form the meddy surface signal in geostrophic balance. For a homogeneous upper layer and the geostrophic approximation, the sea-level anomaly (SLA) over the meddy can be estimated as:

$$\zeta \sim -fR^2\omega_0 g\sqrt{5.5\,e} \sim f^2R^2\Delta H\sqrt{5.5\,e}\,g\tilde{H},$$

where g is gravity acceleration. For our set of parameters ($\Delta H \sim 50$–100 m, $\tilde{H} \sim 700$ m), $\zeta = 3$–6 cm with $R \sim 50$ km, and $\zeta = 6$–12 cm with $R \sim 70$ km. These estimates agree with the elevations observed over some meddies (Oliveira et al., 2000) and are above the altimetric measurement error which is less than 3–4 cm (Fu and Cazenave, 2001).

Vorticity considerations also suggest that at the beginning of meddy propagation (with the upper layer fluid at rest), a cyclonic signal should form on the lee side of the meddy. Observations of meddy Pinball give evidence that at this stage, the cyclonic signal may dominate the anticyclonic surface signature (Fig. 3b). This dominance can also be explained by the potential vorticity conservation. When the meddy starts propagating, the water column in front of the meddy has initially $q_0 = \frac{f}{\tilde{H}}$, which becomes $q_1 = \frac{\omega_{ac}+f}{\tilde{H}-\Delta H}$ when it climbs over the meddy (ω_{ac} is the generated anticyclonic vorticity). The water column initially above the meddy has $q_0 = \frac{f}{\tilde{H}-\Delta H}$, which becomes $q_1 = \frac{\omega_c+f}{\tilde{H}}$ as the column descends the lee side. Thus, the generated anticyclonic relative vorticity: $\omega_{ac} = \frac{f\Delta H}{\tilde{H}}$ should be less than that of the cyclonic signal $\omega_c = \frac{f\Delta H}{\tilde{H}-\Delta H}$. On the contrary, a steadily moving meddy generates only an anticyclonic surface signal, since the isopycnals above, after being pushed upward by the passing meddy, return to their initial depth levels of the upper layer at rest.

4.2 Stratified upper layer

Meddies propagate in the lower part of the permanent thermocline, and the layer above them is not vertically homogeneous. In the stratified case, contrary to the homogeneous case, the potential vorticity change in the upper layer is not only a function of the relative position of two isopycnic surfaces forming the layer boundaries, but also of the mean buoyancy frequency ($N^2 = -\frac{g}{\tilde{\rho}}\frac{\partial \rho}{\partial z}$) of the layer: $q = -\frac{N^2}{g}(f+\omega)$. When the decrease in upper layer thickness is largely compensated by an increase of N, little or no sea-level rise is observed. Dynamically, the acceleration of the divergent motion above the

meddy due to Coriolis force is balanced by the baroclinic radial pressure gradient inside the water column.

On the one hand, the same order of magnitude of the estimate (Eq. 1) and of the observations in Table 1, suggests that the surface signals of strong meddies are only moderately damped by stratification, at least in subtropical latitudes. On the other hand, the rapid decrease of the surface signal of meddy Hyperion as it moved south (Sect. 3) showed that increasing stratification plays an important role in the surface signal damping.

We study the case when the surface signal has already formed over a meddy. Under these conditions, an area where particles are trapped exists above a meddy (Flierl, 1981). Using the quasi-geostrophic approximation with constant f and N, the potential vorticity anomaly is:

$$\tilde{q} - \tilde{q}_0 = \left(\frac{\partial^2}{\partial x^2} + \frac{\partial^2}{\partial y^2} + \frac{f^2}{N^2}\frac{\partial^2}{\partial z^2}\right)\psi,$$

where $\tilde{q}_0$ is a constant background $\tilde{q}$ and ψ is the streamfunction induced by the meddy.

Negative relative vorticity is generated above a meddy to compensate the compression of the upper layer due to the meddy. The ratio of the relative vorticity terms to the stretching term in Eq. (2) is:

$$Bu = \nabla^2\psi\frac{f^2}{N^2}\frac{\partial^2\psi}{\partial z^2} \sim \left(\frac{N\,h}{f\,R}\right)^2.$$

For southern subtropical waters $N = 5\times10^{-3}\,\mathrm{s}^{-1}$, $f = 8\times10^{-5}\,\mathrm{s}^{-1}$, and $\frac{N}{f} \sim 100$, while for northern subtropics $N = 3\times10^{-3}\,\mathrm{s}^{-1}$, $f = 10^{-4}\,\mathrm{s}^{-1}$, and $\frac{N}{f} \sim 30$. Using the characteristics of a meddy surface signal $h = \tilde{H} \sim 700$ m, in the southern subtropics $\tilde{q}$ over a meddy should be conserved for $R \sim 70$ km (compare with Table 2), while in the northern subtropics $\tilde{q}$ over a meddy should be conserved for $R \sim 20$ km. Therefore, in the

northern subtropics we may expect the radius of a surface signal to be close to the radius of a meddy core.

Taking $\tilde{q} - \tilde{q}_0 = 0$ in the layer above the meddy, and constant $\tilde{q}_m = \tilde{q} - \tilde{q}_0$ inside the meddy, we get an equation for the streamfunction anomaly generated by the meddy:

$$\left(\frac{\partial^2}{\partial x^2} + \frac{\partial^2}{\partial y^2} + \frac{\partial^2}{\partial \bar{z}^2}\right)\psi = \tilde{q}_m H(R_m - r), \tag{2}$$

where the rescaled vertical coordinate $\bar{z} = \frac{N}{f}z$, $r = \sqrt{x^2 + y^2 + \bar{z}^2}$ is the distance from the meddy center, R_m is the dynamics radius of the meddy and the Heaviside function is

$$H(R_m - r) = \begin{cases} 1\ (r \le R_m) \\ 0\ (r > R_m) \end{cases}.$$

With the ratio of the vertical to horizontal dimensions in a meddy $\frac{\Delta H}{R_m} = \frac{f}{N}$, the rescaling of the vertical coordinate ($z \to \bar{z}$) leads the meddy to be quasi spherical in the new coordinate system. Shifting from Cartesian to spherical coordinates $(x, y, \bar{z}) \to \boldsymbol{r}(r, \theta, \varphi)$, where θ is the polar angle, counted from the horizontal XY-plane upwards, and φ is the azimuthal angle counted clockwise from the X-axis, the solution of the Poisson equation (Eq. 2) is (Weber and Arfken, 2004):

$$\begin{aligned}\psi(\boldsymbol{r}) &= -\frac{1}{4\pi}\int_{-\pi/2}^{\pi/2}\cos\theta' d\theta' \int_0^{2\pi} d\varphi' \int_0^{\infty} \frac{\tilde{q}_m H(R_m - r')r'^2}{|\boldsymbol{r} - \boldsymbol{r}'|}dr' \\ &= -\frac{1}{4\pi}\int_{\pi/2}^{\pi/2}\cos\theta' d\theta' \int_0^{2\pi} d\varphi' \int_0^{R_m} \frac{\tilde{q}_m r'^2}{|\boldsymbol{r} - \boldsymbol{r}'|}dr', \end{aligned} \tag{3}$$

with the definition of r:

$$\begin{aligned}|\boldsymbol{r} - \boldsymbol{r}'|^2 &= (r'\cos\theta'\cos\varphi' - r\cos\theta\cos\varphi)^2 + (r'\cos\theta'\sin\varphi' - r\cos\theta\sin\varphi)^2 \\ &\quad + (r'\sin\theta' - r\sin\theta)^2 \\ &= r'^2 + r^2 - 2r'r\sin\theta\sin\theta' - 2r'r\cos\theta\cos\theta'(\cos\varphi\cos\varphi' + \sin\varphi\sin\varphi')\end{aligned}$$

We consider the ocean to be isotropic and infinite in all directions around the meddy centre, temporally "forgetting" the sea surface, which is a boundary at finite distance from the meddy. For an isotropic problem, we can arbitrary define θ and φ. It is convenient to set $\theta = \pi/2$, for which $\left|\boldsymbol{r} - \boldsymbol{r}'\right| = \left(r'^2 + r^2 - 2r'r\sin\theta'\right)^{1/2}$. Then Eq. (3) transforms into:

$$\begin{aligned}\psi(\boldsymbol{r}) &= -\frac{\tilde{q}_m}{2}\int_{-\pi/2}^{\pi/2}\int_0^{R_m} \frac{\cos\theta' r'^2}{\left(r'^2 + r^2 - 2r'r\sin\theta'\right)^{1/2}}d\theta' dr' \\ &= \frac{\tilde{q}_m}{2}\int_0^{R_m}\frac{r'}{r}\left\{\left(r'^2 + r^2 - 2r'r\sin\theta'\right)^{1/2}\right\}_{-\pi/2}^{\pi/2} dr' \end{aligned} \tag{4}$$

Since $0 \le r' \le R_m \le r$, the expression in the curly brackets is equal to $\left(r'^2 + r^2 - 2r'r\right)^{1/2} - \left(r'^2 + r^2 + 2r'r\right)^{1/2} = \left|r - r'\right| - \left|r + r'\right| = -2r'$, and Eq. (4) becomes:

$$\psi(\boldsymbol{r}) = -\frac{\tilde{q}_m}{r}\int_0^{R_m} r'^2 dr' = -\frac{\tilde{q}_m R_m^3}{3r} \tag{5}$$

Now we consider the sea-surface to be a horizontal section of our solution at distance $z = H$ from the meddy center (H is the depth of the meddy centre). Then we define

$s = \sqrt{x^2 + y^2}$ as the distance in the horizontal plane counted from the point above the meddy centre and $r = \sqrt{s^2 + b^2}$, where $b = \frac{NH}{f}$. In the quasi-geostrophic approximation, the streamfunction at the sea-surface is equal to $\frac{g\zeta}{f}$, so that the sea-level elevation above a meddy can be expressed as:

$$\zeta(s) = \frac{f\,|\tilde{q}_\mathrm{m}|R_\mathrm{m}^3}{3g\sqrt{s^2 + b^2}} \tag{6}$$

The azimuthal velocity of the surface signal is:

$$v_\theta(s) = \frac{g}{f}\frac{\partial\zeta}{\partial s} = -\frac{|\tilde{q}_\mathrm{m}|R_\mathrm{m}^3}{3}\frac{s}{\left(s^2 + b^2\right)^{3/2}}, \tag{7}$$

and its relative vorticity is:

$$\omega(s) = \frac{\partial v_\theta}{\partial s} + \frac{v_\theta}{s} = -\frac{|\tilde{q}_\mathrm{m}|R_\mathrm{m}^3}{3}\frac{2b^2 - s^2}{\left(s^2 + b^2\right)^{5/2}} \tag{8}$$

An example of the horizontal profiles of the sea-level elevation, azimuthal velocity and vorticity at the sea-surface, Eqs. (6)–(8), are presented in Fig. 5. From Eqs. (6)–(8) it follows that b is the horizontal scale of the surface signal. In particular, the vorticity of the surface signal changes sign at $R = \sqrt{2}\,b$, and v_m reaches its maximum at $s = b/\sqrt{2}$. The dynamical characteristics of the surface signal, for a meddy with $R_\mathrm{m} = 30$ km with a shallow or a deep core, are given in Table 3. The deeper meddies, as well as the meddies observed further south, have larger, but less intense signals.

This result raises two issues for meddy detection at the sea-surface. Firstly, the sea-level anomaly generated by a meddy should obviously be larger than the noise level of the altimetric data. Secondly, the radius of the surface signal should be large enough to intersect the at least one of the adjacent altimetric tracks (Tournadre, 1990). To the

north the diameters of meddy surface signals are comparatively small. This is partly compensated by the altimetric tracks become closer to each other and the AVISO mesh reduces from 29 km at 30° N to 21 km at 50° N. From Eq. (6) it follows that a deep meddy with $R_\mathrm{m} = 20$–30 km, has the SLA of 5–16 cm even 20 km away from the center. Therefore the surface signature of strong meddies should not be intermittent due to being "seeded" in-between the altimetry tracks, while it may become so for weak, small and shallow meddies.

From Table 1, one can conclude that larger ω_0 corresponds to a stronger ω_m. We also note that the $\omega_0/\omega_\mathrm{m}$ ratio follows the R_m/H ratio (Fig. 6a). From Eq. (8), the ratio of the vorticity of the surface signal to that of the meddy is:

$$\frac{\omega(0)}{\omega_\mathrm{m}} = \frac{2}{3}\left[\frac{|\tilde{q}_\mathrm{m}|}{|\omega_\mathrm{m}|}\right]\left(\frac{f\,R_\mathrm{m}}{N\,H}\right)^3 \approx \frac{2}{3}\left[\frac{f}{|\omega_\mathrm{m}|} - 1\right]\left(\frac{f\,R_\mathrm{m}}{N\,H}\right)^3. \tag{9}$$

With $N = \mathrm{const}$, $|\tilde{q}_\mathrm{m}| = \omega_\mathrm{m} + \frac{f^2}{N^2}\frac{\partial^2\psi}{\partial z^2} = \omega_\mathrm{m} + \frac{f^2}{N^2}\frac{1}{f\bar{\rho}}\frac{\partial^2 P}{\partial z^2} = \omega_\mathrm{m} - \frac{f}{N^2}\frac{g}{\bar{\rho}}\frac{\partial\rho}{\partial z} = \omega_\mathrm{m} + f$. The best correspondence between the observed and the predicted (Eq. 9) values of ratio $\omega_0/\omega_\mathrm{m}$ is obtained with $\omega_\mathrm{m} = -0.3f$ (Fig. 6b). The error bars represent mean value of the error, computed assuming the errors in N of 10 %, in H of 100 m and in R_m of 5 km.

Figure 6b shows that the ratio $\omega_0/\omega_\mathrm{m}$ decreases less with an increase of ω_m than predicted by Eq. (9): for the meddis with modulus of relative vorticity smaller than $0.4\,f$ this ratio should be smaller than predicted by Eq. (9), and conversely for the meddies with modulus of relative vorticity larger than $0.4\,f$. The results are not improved when the ratio $\frac{|\tilde{q}_\mathrm{m}|}{|\omega_\mathrm{m}|}$, previously set-up to a constant, varies due to change of ω_m, taken from Table 1. This may mean that for a meddy with large potential vorticity of the core, the relative vorticity plays a relatively smaller role in $\tilde{q}_\mathrm{m}$ as compared to vertical stretching.

The percentage of the explained variance, expressed as the coefficient $R^2 = 1 - \frac{\text{data variance}}{\text{variance of errors}} = 93\,\%$, when meddy Ceres is excluded and when the linear trend of the $\omega_0/\omega_\mathrm{m}$ ratios (for prediction versus observation) is eliminated. At the time of the in situ observations (presented in Table 1) the surface signal of meddy Ceres is affected by

the alignment with a surface anticyclone (Tychensky and Carton, 1998), and should not be described by Eq. (9). The backtracking of the meddy surface signal identified this anticyclone as a detached meander of the Azores Current (Bashmachnikov et al., 2009a).

With mean $\omega_m = -0.3f$, the maximum value of SLA at the centre of the surface signal is:

$$\zeta(0) = \frac{|\tilde{q}_m|}{3g}\frac{f^2 R_m^3}{NH} \sim 0.024\frac{f^3 R_m^3}{NH} \quad (10)$$

From Eq. (10), the intensity of the surface signal is most sensitive to the dynamic radius of the underlying meddy.

5 Analysis of meddy surface signals in the Northeastern Atlantic Ocean

The time evolution of the meddy surface signatures is now analysed taking into account our theoretical elements of the previous section (Fig. 7).

Considering slow, and mostly zonal, meddy propagations, the variation of the surface signals due to the variation of stratification should be visible over time scales of a season or longer. But at such time-scales the characteristics of a meddy core may also change. For instance, during a year of observations, the RAFOS floats trapped in Hyperion deepened by 100 m, suggesting a corresponding increase of H. The rather high dispersion of the RAFOS position relative to the meddy centre makes it difficult to reliably assess a small decrease of the meddy radius with time (if any). Repeated observations of meddy Sharon (Hebert et al., 1990) showed that its dynamical radius decreased by 9 km during a year of observations. To compute the time evolution of the meddy surface signatures in Fig. 7, we assumed that the meddy radii decreased by 5 km per year.

Figures 6 and 7 show that expressions (9)–(10) adequately describe the intensity and time evolution of the surface signals of meddies, though slightly overestimate the

intensity of the sea-level anomalies over meddies with comparatively low ω_m, as has been noted earlier (cf. Fig. 6).

From November 1993 to November 1994 Hyperion moved south by six degrees of latitude. Its surface signal notably decreased (Figs. 2 and 7), a priori affected by both the decrease of meddy-core intensity and the increase of stratification. After May 1994, i.e. after the meddy crossed 30° N, its surface signal did not exceed 5 cm any longer, and it became difficult to distinguish it from the background noise. The predictions correctly describe the overall trend in the intensity of the surface signal of Hyperion, although fail to explain rapid episodic drops of the signal intensity. Note that those variations happened when the meddy crossed the Azores Current (October 1993) and interacted with a cyclone (December 1993–January 1994), i.e. when the meddy surface signal is influenced by the intensive background dynamic fields.

The evolution of meddy Ceres was specific (Richardson et al., 2000) and the information on its characteristics does not allow a correct description of the variations of its surface signal. At the beginning of its study, Ceres was aligned with a surface anticyclone (Tychensky and Carton, 1998) and the SLA did not represent the meddy surface signal proper. Later on, the meddy rapidly crossed the Azores Current, an event during which the surface signal got lost (Bashmachnikov et al., 2009a). Sharp variations of the radius of rotation of RAFOS floats during this period suggest that, during this crossing, the core of this weak meddy underwent destructive changes.

Meddies Encelade and Zoe followed a zonal trajectory, which could have allowed the observation of the seasonal influence of stratification. But Encelade was trapped by the southern boundary of the Azores Current; therefore, its surface signal was also determined by this effect. The fact that Eq. (10) works reasonably well in description of its intensity and dynamics, indicates that the influence of the meddy dominated the evolution of its surface signature, compared with the influence of the meanders of the Azores Current (see also Bashmachnikov et al., 2009a, 2012). The signal over Encelade showed a 15 % decrease from winter to summer.

The characteristics of meddy Zoe core are not described in literature in sufficient detail for our analysis. Here, we used $H = 1200$ m, $R_m = 30$ km, $\omega_m = -0.2\,f$ (Richardson and Tychensky, 1998). The variations of the SLA above Zoe in October–December 1995 were not related with the surface signature of the meddy itself but they were due to the influence of another anticyclone which approached Zoe from the north (see Sect. 3). The proper surface signal of Zoe during this period is better seen in the vorticity field (Fig. 1b).

Initially, the surface signal of the meddy Pinball was weaker than expected, since the meddy was in its formation stage. Its surface signal reached the estimated intensity only in April 1994, when the meddy started moving westward (Fig. 3a, b). At the end of its registered journey, the increase in surface signal of Pinball resulted from the increase of the meddy radius and from the decrease of the meddy core depth; these two changes were due to the merger of Pinball with another meddy (with a shallower core) in June 1994 (Pingree, 1995). The surface signal then grew above the value predicted with the original characteristics of Pinball.

Meddies B2 and Aska (B1) were observed during a merging process: B1 was absorbed by the stronger meddy B2 (Schultz Tokos et al., 1994). Acceleration and deformation of the core of B1 during the merging may explain the observed deviation of the intensity of its surface signal from Eq. (10).

The gridded AVISO products allow a reliable identification of a mesoscale signal when $\zeta \geq 4$ cm and when this signal does not entirely lie between the ground tracks of the satellites (Fu and Cazenave, 2001). For a mesoscale structure lying exactly on the ground track of an altimetric satellite, the accuracy improves to 2 cm. Taking either one of these criteria as the critical value, we can evaluate where meddies with certain characteristics may be identified in AVISO altimetry. Based on the Figs. 6 and 7, we chose ±2 cm error bars. The results are presented on Fig. 8. It follows from Fig. 8 that in the main meddy propagation path, around 36–38° N, (Shapiro and Meschanov, 1996), meddies with dynamic radii of 20 km will be detectable at the surface, but their signal should be weak and fairly intermittent. Such small meddies should quickly loose

their surface signatures if they take a southern path, e.g. along the coast of Africa (Hebert et al., 1990). Meddies with $R_m = 30$ km with both shallow and deep cores, are detectable in both subtropics and northern tropics, at least as far as 25–30° N. This latter prediction corresponds well to the evolution of the surface signal of meddy Hyperion, which became weak and often intermittent south of 30° N.

Figure 8 also shows that the isolines of the sea surface elevation ζ in the Eastern North Atlantic are nearly zonal; therefore we can easily compute critical latitudes, south of which a meddy cannot be identified in altimetry, in the $H - R_m$ plane (Fig. 9). In particular, Fig. 9 shows that a meddy with $R_m = 10$ km is not detectable in altimetric data anywhere in this region, while meddies with $R_m = 15$ km may be episodically seen north of 40° N.

6 Conclusions

In-situ (Table 1) and altimetric (Table 2) observations clearly indicate that most of the registered meddies showed a vertical alignment with an anticyclonic eddy at the sea surface (keeping in mind that the spatial precision allowed by the gridded AVISO altimetry products is ±15 km). This surface eddy was between 50 and 100 km in diameter and its surface elevation/relative vorticity anomalies peaked near the meddy center, where they reached 5–15 cm/−0.05– −0.15f, respectively. The surface signal, as a rule sufficiently strong to be detected in altimetry, was typically smaller than that of strong surface anticyclones, as for example, the meanders of the Azores Current (Table 2).

Drifting meddies lift isopycnals above and in front of them and return to the initial position behind them, thus generating anticyclonic surface vorticity anomalies. Potential vorticity conservation also suggests that when a meddy starts drifting, rapidly accelerates, or abruptly changes direction, a surface cyclone can also be generated at the lee side of a meddy. A clear cyclonic signal was formed when meddy Pinball started its westward propagation away from the coast. Near the coast the formation of the cyclonic signal may also have resulted from the interaction of meddy Pinball with a southward

surface flow (Aiki and Yamagata, 2004). At the same time, the surface cyclone did not couple with the meddy surface signal as predicted by Aiki and Yamagata's model; on the contrary, it stayed in its region of formation (Richardson et al., 2000), more in accordance with the mechanism suggested here.

The surface signal of a meddy may be strongly damped by the upper ocean stratification. In a stratified ocean, the energy of this signal is partitioned between baroclinic and barotropic components, and, in the limiting case, may not reach the sea-surface. The vertical damping effect is mostly a function of $\frac{H}{R_m}$. Our criteria (Eqs. 6–10) provide a fair estimate of the observed variation of surface signals above meddies. But they also slightly overestimate the intensity of the surface signals for meddies with low ω_m, while they underestimate it for meddies with high ω_m.

The background conditions enter these criteria via the $\frac{N}{f}$ ratio. This allows the calculation of sea-surface detection conditions for various meddy-core parameters. With the present accuracy of altimetric data, remote detection of meddies in subtropics is possible when the meddy cores are larger than 10–15 km, while in tropics only very large meddies, with R_m between 25 and 35 km, are detectable. Seasonality in the upper layer stratification affects the intensity of the signal, but the range of the seasonal variation should not exceed 2–4 cm.

The decrease in signal intensity with time results not only from the southwestward meddy drift, but also from the variation of characteristics of meddy cores. Gradual or drastic dissipation of the cores results in decrease or loss of the signals. Conversely, meddy merger with another meddy results in an increase of the intensity of the surface signal.

A number of effects affecting the meddy signal itself were not taken into account here. Besides alignment with an existing surface anticyclone, a mean background flow may shed the surface signal away. This may be the cause for the decreasing intensity of the surface signals of the meddies which cross the Azores Current (Hyperion, Ceres). For these meddies the effect of the background flow should also be considered in detail (Vandermeirsch et al., 2003a,b). When interacting with a cyclone, a meddy may "dive"

under the cyclone, losing its surface signal (Richardson et al., 2000; Carton et al., 2010). When a meddy propagates with β-drift velocities, resonance with the baroclinic Rossby waves may heavily damp the surface signals. Such effects should be studied with very high resolution models of the Northeastern Atlantic Ocean.

Acknowledgements. I. B. acknowledges the contract C2008-UL-CO-3 of Ciencia 2008 between Foundation for Science and Technology (FCT) and the University of Lisbon (UL) and Center of Oceanography of the University of Lisbon. X. C. acknowledges the contract REI COMINO from DGA.

References

Aiki, H. and Yamagata, T.: A numerical study on the successive formation of meddy-like lenses, J. Geophys. Res., 109, C06020, doi:10.1029/2003JC001952, 2004.

Armi, L., Hebert, D., Oakey, N., Price, J. F., Richardson, P. L., Rossby, H. T., and Ruddick, B.: The history and decay of a Mediterranean salt lens, Nature, 333, 649–651, 1988.

Armi, L., Hebert, D., Oakey, N., Price, J. F., Richardson, P. L., Rossby, H. T., and Ruddick, B.: Two years in the life of a Mediterranean salt lens, J. Phys. Oceanogr., 19, 354–370, 1989.

Assenbaum, M. and Reverdin, G.: Near real-time analyses of the mesoscale circulation during the POMME experiment, Deep-Sea Res. Pt. I, 52, 1345–1373, 2005.

AVISO altimeter products, produced by Ssalto/Duacs and distributed by Aviso, with support from CNES, available at: http://www.aviso.oceanobs.com, last access: 1 November 2011.

Bashmachnikov, I., Machin, F., Mendonca, A., and Martins, A.: In-situ and remote sensing signature of meddies east of the Mid-Atlantic ridge, J. Geophys. Res., 114, C05018, doi:10.1029/2008JC005032, 2009a.

Bashmachnikov, I., Mohn, C., Pelegrí, J. L., Martins, A., Machín, F., Jose, F., and White, M.: Interaction of Mediterranean water eddies with Sedlo and Seine seamounts, Subtropical Northeast Atlantic, Deep-Sea Res. Pt. II, 56, 2593–2605, 2009b.

Bashmachnikov, I., Boutov, D., Dias, J., Aguiar, A., and Monteiro, J. H.: Surface signature of a meddy while interacting with the Azores current, in: Geophysical Research Abstracts, Vol. 14, EGU General Assembly, Vienna, Austria, 24–27 April 2012, EGU2012-6152-1, 2012.

Bower, A. S., Armi, L., and Ambar, I.: Lagrangian observations of meddy formation during a Mediterranean undercurrent seeding experiment, J. Phys. Oceanogr., 27, 2545–2575, 1997.
Carton, X. J., Flierl, G. R., and Polvani, L. M.: The generation of tripoles from unstable axisymmetric isolated vortex structures, Europhys. Lett., 9, 339–344, 1989.
Carton, X. J., Cherubin, L., Paillet, J., Morel, Y., Serpette, A., and Le Cann, B.: Meddy coupling with deep cyclone in the gulf of Cadiz, J. Marine Syst., 32, 13–42, 2002.
Carton, X. J., Daniault, N., Alves, J., Cherubin, L., and Ambar, I.: Meddy dynamics and interaction with neighboring eddies southwest of Portugal: observations and modelling, J. Geophys. Res., 115, C06017, doi:10.1029/2009JC005646, 2010.
Flierl, G. R.: Particle motions in large-amplitude wave fields, Geophys. Astro. Fluid, 18, 39–74, 1981.
Flierl, G. R.: Rossby-wave radiation from a strongly nonlinear warm eddy, J. Phys. Oceanogr., 14, 47–58, 1984.
Fu, L.-L. and Cazenav, A. (Eds.): Satellite Altimetry and Earth Sciences – A Handbook of Techniques and Applications, International Geophysics Series 69, Academic Press, London, 1–463, 2001.
Hebert, D. L.: A Mediterranean Salt Lens, Ph. D. thesis, Dalhousie University, Halifax, Nova Scotia, 187 pp., 1988.
Hebert, D., Oakey, N., and Ruddick, B.: Evolution of a Mediterranean salt lens: scalar properties, J. Phys. Oceanogr., 20, 1468–1483, 1990.
Isern-Fontanet, J., Garcia-Ladona, E., and Font, J.: Identification of marine eddies from altimetric maps, J. Atmos. Ocean. Tech., 20, 772–778, 2003.
Käse, R. H., Beckmann, A., and Hinrichsen, H. H.: Observational evidence of salt lens formation in the Iberian basin, J. Geophys. Res., 94, 4905–4912, 1989.
Le Cann, B., Assenbaum, M., Gascard, J.-C., and Reverdin, G.: Observed mean and mesoscale upper ocean circulation in themidlatitude Northeast Atlantic, J. Geophys. Res., 110, C07S05, doi:10.1029/2004JC002768, 2005.
Legras, B. and Dritschel, D. G.: Vortex stripping and the generation of high vorticity gradients in two-dimensional flows, Appl. Sci. Res., 51, 445–455, 1993.
Mariotti, A., Legras, B., and Dritschel, D. G.: Vortex stripping and the erosion of coherent structures in two-dimensional flows, Phys. Fluids, 6, 3954–3962, 1994.

Martin, A. P., Richards, K. J., Law, C. S., and Liddicoat, M.: Horizontal dispersion within an anticyclonic mesoscale eddy, Deep-Sea Res. Pt. II, 48, 739–755, 2001.
Oliveira, P. B., Serra, N., Fiúza, A. F. G., and Ambar, I.: A study of meddies using simultaneous in situ and satellite observations, in: Satellites, Oceanography and Society, Elsevier Oceanography Series 63, Elsevier, Amsterdam, 125–148, 2000.
Paillet, J., Le Cann, B., Carton, X., Morel, Y., and Serpette, A.: Dynamics and evolution of a northern meddy, J. Phys. Oceanogr., 32, 55–79, 2002.
Pingree, R. D.: The droguing of meddy Pinball and seeding with ALACE floats, J. Mar. Biol. Assoc. UK, 75, 235–252, 1995.
Pingree, R. D. and Le Cann, B.: Structure of a meddy (Bobby 92) southeast of the Azores, Deep-Sea Res. Pt. I, 40, 2077–2103, 1993a.
Pingree, R. D. and Le Cann, B.: A shallow meddy (a Smeddy) from the secondary mediterranean salinity maximum, J. Geophys. Res., 98, 20169–20185, 1993b.
Richardson, P. L. and Tychensky, A.: Meddy trajectories in the Canary Basin measured during the Semaphore experiment, 1993–1995, J. Geophys. Res., 103, 25029–25045, 1998.
Richardson, P. L., Walsh, D., Armi, L., Schröder, M., and Price, J. F.: Tracking three meddies with SOFAR floats, J. Phys. Oceanogr., 19, 371–383, 1989.
Richardson, P. L., Bower, A. S., and Zenk, W.: A census of meddies tracked by floats, Progr. Oceanogr., 45, 209–250, 2000.
Schultz Tokos, K., Hinrichsen, H. H., and Zenk, W.: Merging and migration of two meddies, J. Phys. Oceanogr., 24, 2129–2141, 1994.
Serra, N. and Ambar, I.: Eddy generation in the Mediterranean undercurrent, Deep Sea Res. Pt. I, 49, 4225–4243, 2002.
Shapiro, G. I. and Meschanov, S. L.: Spreading pattern and mesoscale structure of Mediterranean outflow in the Iberian basin estimated from historical data, J. Marine Syst., 7, 337–348, 1996.
Stammer, D., Hinrichsen, H. H., and Käse, R. H.: Can meddies be detected by satellite altimetry?, J. Geophys. Res., 96, 7005–7014, 1991.
Tournadre, J.: Sampling of oceanic rings by satellite radar altimiter, J. Geophys. Res., 95, 693–698, 1990.
Tychensky, A. and Carton, X.: Hydrological and dynamical characteristics of meddies in the Azores region: a paradigm for baroclinic vortex dynamics, J. Geophys. Res., 103, 25061–25079, 1998.

Vandermeirsch, F. O., Carton, X. J., and Morel, Y. G.: Interaction between an eddy and a zonal jet. Part I. One and a half layer model, Dynam. Atmos. Oceans, 36, 247–270, 2003a.
Vandermeirsch, F. O., Carton, X. J., and Morel, Y. G.: Interaction between an eddy and a zonal jet. Part II. Two and a half layer model, Dynam. Atmos. Oceans, 36, 271–296, 2003b.
Van Geffen, J. H. G. M. and Davies, P. A.: A monopolar vortex encounters an isolated topographic feature on a beta-plane, Dynam. Atmos. Oceans, 32, 1–26, 2000.
Weber, H. J., Arfken, G. B.: Essential Mathematical Methods for Physicists, Elsevier, Amsterdam, 1–932, 2004.
WOA09: World Ocean Atlas 2009, available at: http://www.nodc.noaa.gov/OC5/WOA09/pubwoa09.html (last access: 1 November 2011), compiled by Locarnini, R. A., Mishonov, A. V., Antonov, J. I., Boyer, T. P., Garcia, H. E., Baranova, O. K., Zweng, M. M., and Johnson, D. R., 2010, Volume 1: Temperature. Levitus, S., Ed. NOAA Atlas NESDIS 61, US Government Printing Office, Washington, DC, 184 pp. and Antonov, J. I., Seidov, D., Boyer, T. P., Locarnini, R. A., Mishonov, A. V., Garcia, H. E., Baranova, O. K., Zweng M. M., and Johnson, D. R., 2010. Volume 2: Salinity, edited by: Levitus, S., NOAA Atlas NESDIS 69, US Government Printing Office, Washington, DC, 184 pp., 2009.

Table 1. Characteristics of surface signatures of various meddies, derived from in situ observations (the meddies are sorted from weaker to more intense ones): $v_m(\omega_m)$ and $v_0(\omega_0)$ are the maximum azimuthal velocity (vorticity) in the meddy core and in its surface signal, respectively.

Meddie's name, position, time of observations	H, m/R_m, km	v_m, cm s^{-1}	v_0, cm s^{-1}	$\Delta\zeta$, cm	$\lvert\omega_m\rvert/f$	$\lvert\omega_0\rvert/f$	ω_0/ω_m, %	Reference, Instrumentation*
Ceres, 36° N, 24° W, 07–09.93, 0 m	1000 / 30	12	23	13	0.13	0.12	96 %	Tychensky and Carton (1998), CTD, XBT, SF, SLA; (south of the Azores)
Encelade, 33° N, 21° W, 10–11.93, 0 m	1000 / 35	14	8	5	0.13	0.04	29 %	Tychensky and Carton (1998), CTD, XBT, SF, SLA; (south of the Azores)
Hyperion, 35° N, 28° W, 07.93, 0 m	900 / 35	20	13	8	0.18	0.06	33 %	Tychensky and Carton (1998), CTD, XBT, SF, SLA; (south of the Azores)
Ulla, 45° N, 12° W, 04.97, 0 m	1100 / 15	18	8	2	0.38	0.08	22 %	Paillet et al. (2002), CTD, XBT, LADCP, RAFOS, DDB, SF
Pinball (A3), 01.94, 37–38° N, 10–12° W, 0 m	1000 (700–1200)/ 20 (10–35)	25 (20–30)	15 (10–20)	6	0.39	0.12	30 %	Pingree (1995), Oliveira et al. (2000), RAFOS, SF, SLA, SST
Bobby92, 35° N, 23° W, 03.92, 0 m	1100 / 22	30	15	6	0.43	0.11	25 %	Pingree and Le Cann (1993b), CTD, ADCP, buoys
B2, 38° N, 13° W, 04–05.91, 100 m	1300 / 25	31	18	8	0.39	0.11	29 %	Schultz Tokos et al. (1994), CTD, RAFOS, SF
Aska (B1), 38° N, 13° W, 04–05.91, 100 m	1000 / 18	27	15	5	0.47	0.13	28 %	Schultz Tokos et al. (1994), CTD, RAFOS, SF
Smeddy, 36° N, 9° W, 03.92, 0 m	700 / 12	20	8	2	0.52	0.10	20 %	Pingree and Le Cann (1993a), CTD, XBT, PF, SST
A2/05, 41° N, 17° W, 09.00 & 40° N, 19° W, 02.01, 100 m	no data	15	13	4	0.23	0.10	43 %	Le Cann et al. (2005), Assenbaum et al. (2005), CTD, RAFOS, PF, SF; (Azores-Biscay Rise)
A2/00, 02–03.94, 37–38° N, 10–12° W, 0 m	no data	20	17	5	0.30	0.13	43 %	Oliveira et al. (2000), RAFOS, SF, SLA
A1/00, 05–06.94, 37–38° N, 10–12° W, 0 m	no data	23	23	7	0.35	0.17	50 %	Oliveira et al. (2000), RAFOS, SF, SLA
AVERAGE				6	0.30	0.10	32 %	

* Instrumentation, showing deep and/or surface signatures: CTD – conductivity-temperature-depth profilers, XBT – expandable bathythermograph profilers, RAFOS, PF and DDB – deep floats (free floating, profiling of deep-drogued), SF – surface floats, SLA – sea-level anomalies, SST – sea-surface temperature.
H is the depth of a meddy core, R_m is dynamic radius, vorticity is estimated as $\omega_m = 2\sqrt{e}1.2\, v_m/R_m$, sea-level anomaly is estimated from the quasi-geostrophic approximation: $\Delta\zeta = (fV_s + V_s^2/2) * R_m/g$. For the surface signal R_m is doubled in accordance with observations.

Table 2. Mean vorticity values (normalized by f) at various distances from the centers of meddies, as calculated from RAFOS floats; ω_0 and $\omega_{0\,\min}$, are the average and the peak negative vorticity over the 100 km around the meddy center.

Meddy (time of observations)	Zoe (Sep 94–Feb 95)	Hyperion (Jul 93–Jun 94)	Encelade (Nov 93–May 94)	Ceres (Oct 93–Jan 94)	Pinball (Jan–Sep 94)
ω/f at 20 km	−0.07±0.02	−0.06±0.03	−0.08±0.02	−0.05±0.06	−0.02±0.02
ω/f at 45 km	−0.03±0.01	−0.03±0.02	−0.06±0.01	−0.03±0.03	−0.01±0.01
ω/f at 75kn	0.01±0.01	−0.01±0.01	−0.02±0.01	−0.01±0.01	−0.00±0.01
mean background ω/f in 4° × 4° square	−0.005±0.003	0.001±0.005	0.004±0.002	0.000±0.003	0.001±0.001
ω_0/ω_m, %	20 ± 5 %*	40 ± 20 %	35 ± 5 %	45 ± 45 %	20 ± 35 % **
$\omega_0 < 0, \omega_{0\min} < 0$, in % of time of observations	100, 100 %	93, 94 %	100, 100 %	70, 100 %	78, 100 %
% of time when the peak negative vorticity in 4° × 4° square is situated over the meddy	20 %	35 %	90 %	40 %	20 %

* Relative vorticity of the core was set constant and equal to $-0.2f$;
** Includes initial period of meddy stagnation, when anticyclonic signal has not been formed yet.

Table 3. Characteristics of the surface signals for a meddy with the R_m = 30 km and $|\tilde{q}_m| = 0.7f$ in northern subtropics (N/f = 30) and southern subtropics (N/f = 100).

region	H_m, m	$\zeta(0)$, cm	Radius of v_θ = max, km	Radius of ω = 0, km
N subtropics	600	35	25	35
	1100	19	23	47
S subtropics	600	8	37	74
	1100	4	68	136

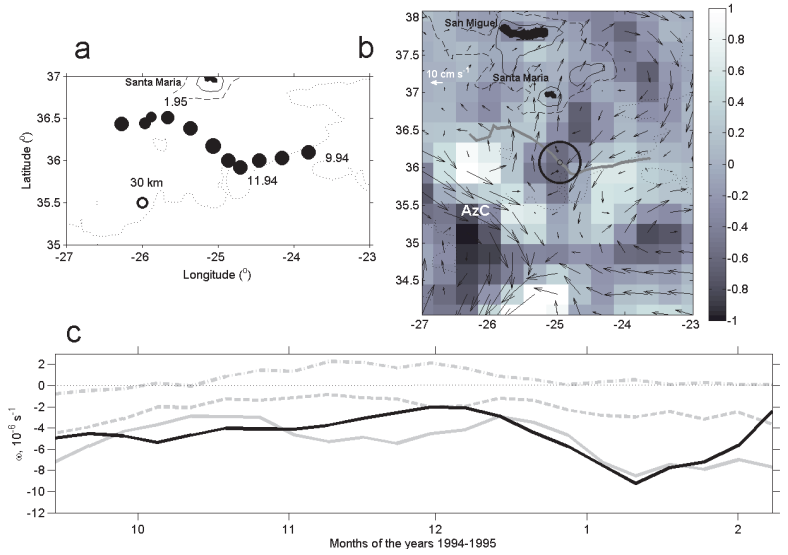

Fig. 1. Temporal evolution of the characteristics of meddy Zoe and of its surface signature. **(a)** Track of Zoe with month-year marked. The width of the circle represents the RAFOS float rotation radius in km. Black lines mark depth contours: 1000 m (solid), 2000 m (dashed), 4000 m (dotted). **(b)** Example of surface vorticity field ($10^{-5}\,s^{-1}$, colour) and geostrophic currents ($cm\,s^{-1}$) derived from AVISO altimetry with the meddy position marked with a black ring at 22 November 1994. The grey line is the track of meddy center: the meddy moved from the right (13 September 1994) to the left (10 February 1995) of the plot. **(c)** Time evolution of 1-month sliding average of meddy peak relative vorticity (solid black line, $10^{-6}\,s^{-1}$), of the mean relative vorticity of the meddy surface signal at $r < 20$ km (solid thin grey line, $10^{-6}\,s^{-1}$), at $r \sim 20$–60 km (dashed thin grey line, $10^{-6}\,s^{-1}$), at $r \sim 60$–80 km (dash-dotted thin grey line, $10^{-6}\,s^{-1}$).

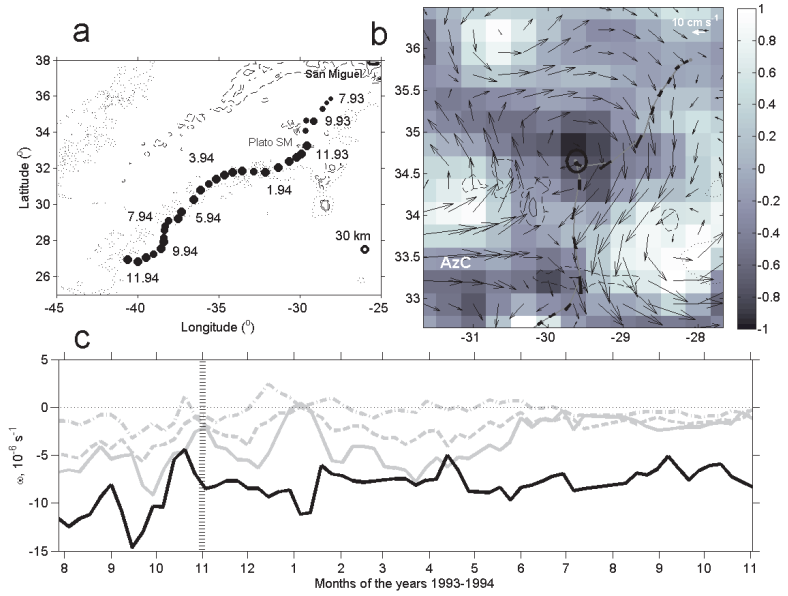

Fig. 2. Same as Fig. 1, but for meddy Hyperion; **(b)** shows the AVISO derived currents on 22 September 1993.

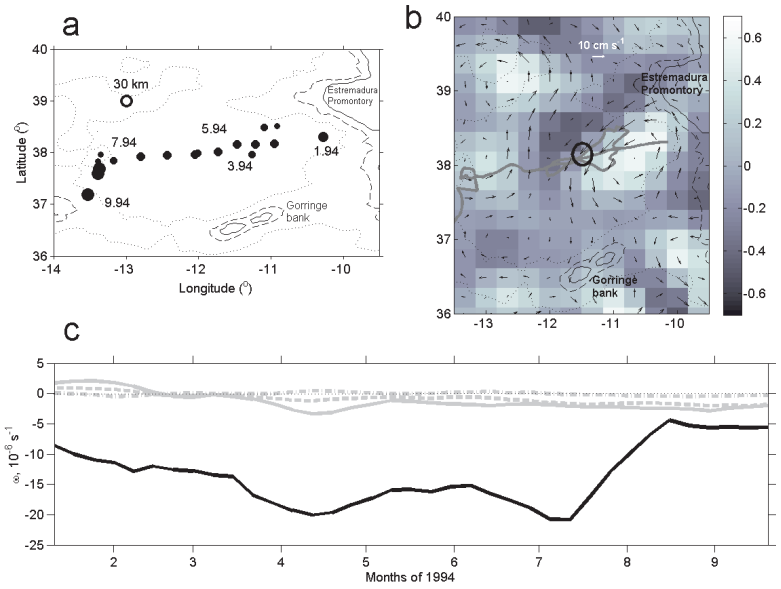

Fig. 3. Same as Fig. 1, but for the meddy Pinball; **(b)** shows the AVISO derived currents on 4 May 1994.

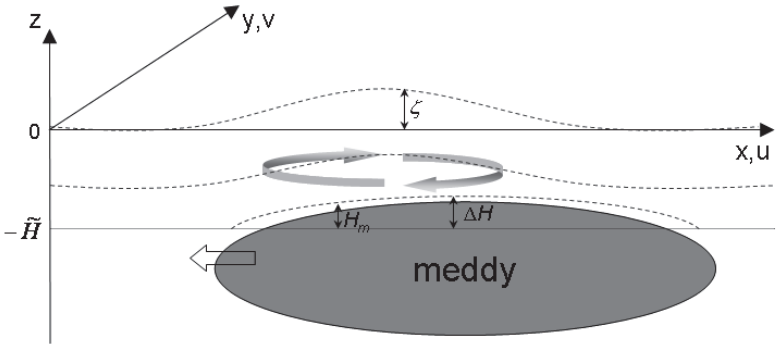

Fig. 4. Schematic view of generation of a surface signal by a meddy.

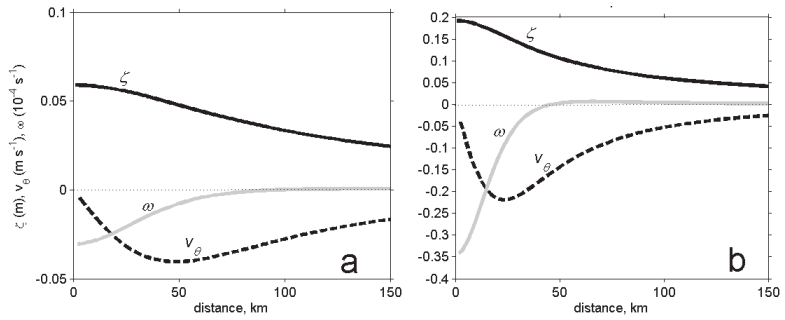

Fig. 5. Radial profiles of ζ (m, solid black line), v_θ (m s^{-1}, dash line) and ω (10^{-4} s^{-1}, solid grey line) of the surface signal of a meddy with R_m = 30 km, H = 1100 m and $|\tilde{q}_m| = 0.7f$; **(a)** in the northern subtropics, **(b)** in the southern subtropics.

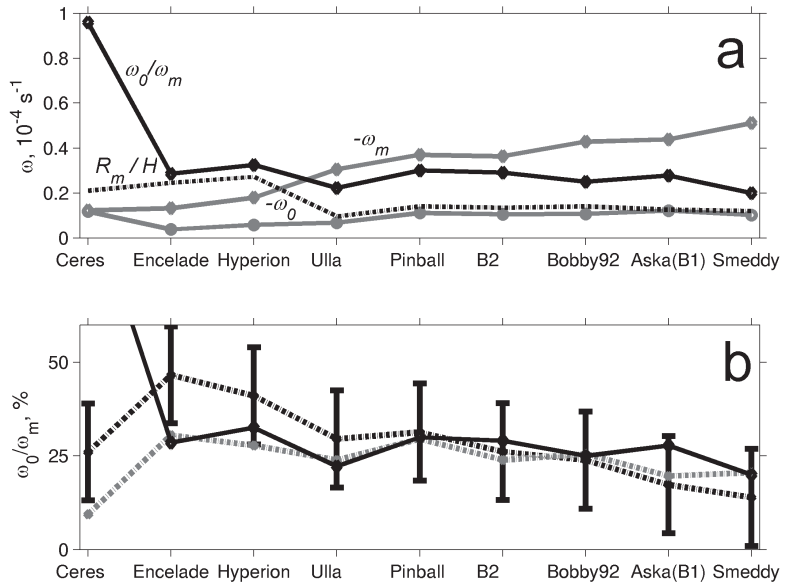

Fig. 6. (a) Variations of meddy-core (ω_m – thick grey line with triangles) and surface (ω_0 – grey line with circles) peak relative vorticity, ratio ω_0/ω_m (solid black line) and R_m/H ratio (dashed black line, not in the scale). The x-axis gives the names of the meddies listed in Table 2. **(b)** Ratio the observed ω_0/ω_m (solid line), predicted from Eq. (9) (dash-dotted black line) and predicted from Eq. (9) with the trend removed (dash-dotted grey line). The buoyancy frequency was obtained from the climatic monthly mean density fields (WOA09).

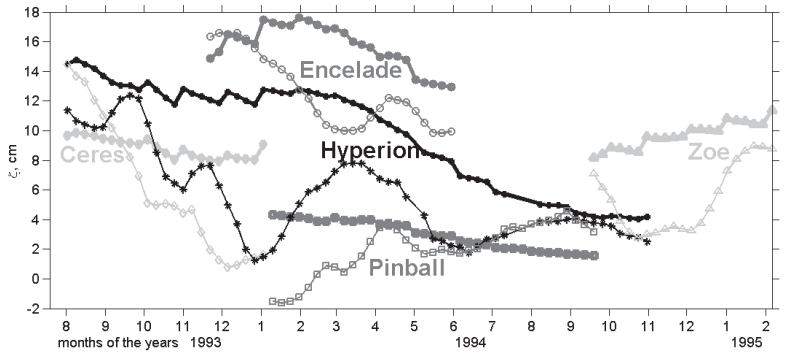

Fig. 7. Sea-level anomalies over meddies (cm) computed from AVISO altimetry (thin lines) and expression (10) (thick lines) for meddies Hyperion (stars, black line), Encelade (circles, dark grey), Pinball (squares, dark grey), Ceres (diamonds, light grey) and Zoe (triangles, light grey). The buoyancy frequency was obtained from the climatic monthly mean density fields (WOA09).

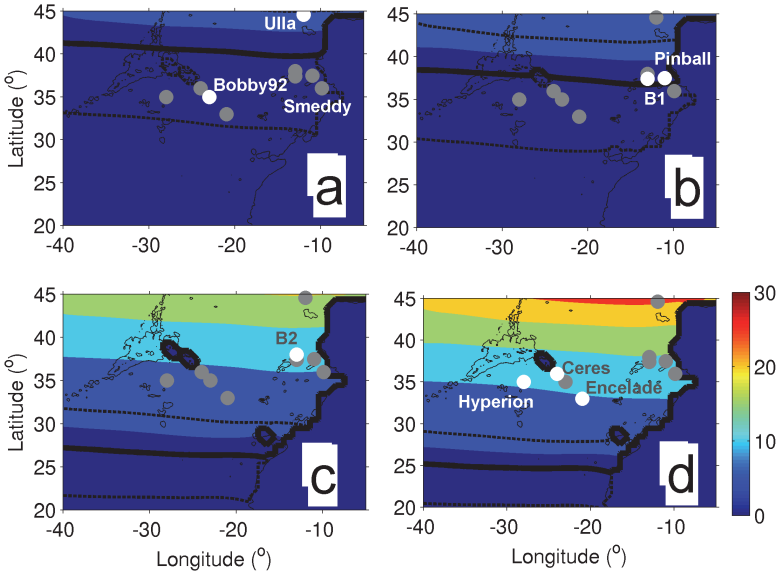

Fig. 8. Sea-level anomaly (cm): **(a)** $H = 1100$ m, $R_m = 20$ km; **(b)** $H = 800$ m, $R_m = 20$ km, **(c)** $H = 1100$ m, $R_m = 30$ km, **(d)** $H = 800$ m, $R_m = 30$ km. The thick black line marks the critical value $\zeta = 4$, while its position will vary within the limits of the dashes lines when a ± 2 cm interval for detectable signals is introduced. The buoyancy frequency was obtained from the mean climatic density field (WOA09). Grey circles mark the meddies described in the text (Table 1); white circles are the meddies with the $H - R_m$ characteristics close to the ones presented at the respective panel.

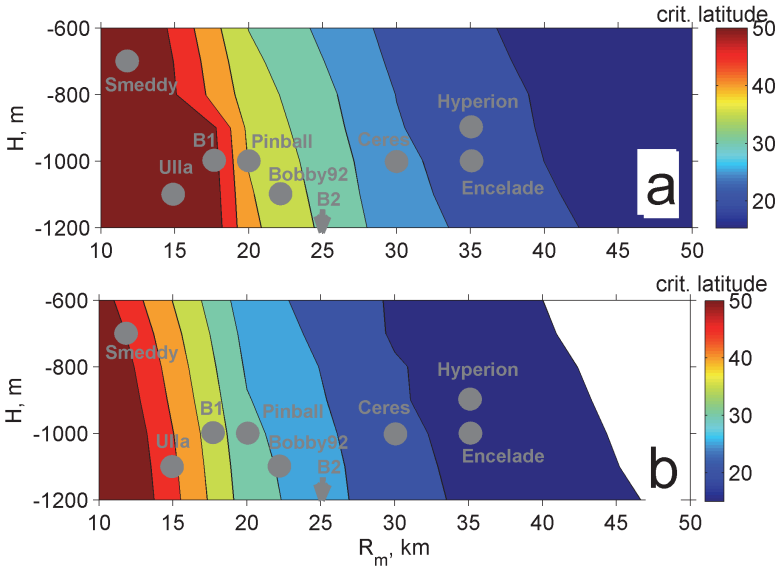

Fig. 9. Critical latitudes, presented as a function of meddy core depth H and of its dynamic radius R_m, for $\zeta < 4$ cm **(a)** and $\zeta < 2$ cm **(b)**. Meddies with given $[H, R_m]$ set of characteristics are detectable in AVISO altimetry data at latitudes north of those presented in the graph. The buoyancy frequency was obtained from the mean climatic density field (WOA09). Grey circles mark the meddies described in the text (Table 1).